Mining, Metallurgy & Exploration (2023) 40:57–64
https://doi.org/10.1007/s42461-022-00705-x

Isothermal Reduction Kinetics of Copper Slag-Biomass Composite Pellets

Shuai Li[1,2] · Hui Shu[3,4,5] · Hongling Wang[3,4,5] · Di Wu[3,4,5]

Received: 1 September 2022 / Accepted: 10 November 2022 / Published online: 23 November 2022

Abstract
Isothermal reduction experiments on carbon-bearing pellets of copper slag were investigated by the thermogravimetric method with biomass carbon as a reducing agent. The results indicated that the reduction process of copper slag-biomass composite pellets was dominated by gas phase diffusion, and the apparent activation energy was 88.44 kJ/mol. In the temperature range from 1000 to 1200 °C, the metallization rate of pellets increased with increasing temperature, and the maximum metallization rate was 78.4%. The optimal reduction temperature of CSBCP (copper slag-biomass composite pellets) was 1200 °C.

Keywords Copper slag · Carbothermal reduction · Kinetics

1 Introduction

Copper slag, produced in the process of copper smelting, is rich in iron oxides, silicates, and sulfides [1]. According to different raw material grades, processes, and operating levels, approximately 2.2 to 3 tons of copper slag is generated for every ton of copper produced [2]. In terms of quantity, copper slag is only second to red mud in non-ferrous smelting slag. It is estimated that the amount of copper slag discharged into the environment in China is as high as 19 to 26.7 million tons every year [3]. However, only a few part of the copper slag has been used by building materials [4], paving materials [5], rust removers [6], etc. Up to now, its cumulative stockpile has exceeded 200 million tons.

The most abundant element in copper slag is Fe/O/Si, among which the iron content is usually 35–45% [7], while the average grade of iron ore in China is only 30%. China is a big country of iron and steel, and its dependence on foreign iron ore is more than 80%. Therefore, it is very necessary and urgent to recover the iron resources in copper slag. Researchers all over the world have carried out a lot of work on the recovery of iron from copper slag and have achieved remarkable results, such as direct magnetic separation, reduction of roasting-magnetic separation, oxidative roasting-magnetic separation, high-temperature smelting reduction, and wet leaching [6]. However, the actual utilization rate of iron in copper slag is less than 1%. The main reason is that iron in copper slag exists in the fayalite phase with a relatively stable structure. In traditional beneficiation methods, such as flotation, the recovery rate of iron is only about 25–30%. Although the reduction method has a high iron recovery rate, it has the disadvantages of high-energy consumption and large consumption of reducing agent, making it economically uneconomical. So, it has not yet achieved commercial application. Despite the shortcomings in the

✉ Hui Shu
Shuhuineu@163.com

✉ Hongling Wang
286890070@qq.com

Shuai Li
lishuai.neu@foxmail.com

1 Environmental Protection and Energy Conservation Group Co., Ltd.of CHINALCO, Beijing 101300, China

2 Institute of Environmental Protection and Energy Conservation, Central Research Institute of Chinalco, Beijing 101300, China

3 Institute of Resources Utilization and Rare Earth Development, Guangdong Academy of Sciences, Guangzhou 510650, China

4 State Key Laboratory of Rare Metals Separation and Comprehensive Utilization, Guangzhou 510651, China

5 Guangdong Key Laboratory of Mineral Resources Development and Comprehensive Utilization, Room 227, Ziyuan Building, No.363, Changxing Road, Tianhe District, Guangzhou 510651, Guangdong Province, China

Table 1 Chemical composition of copper slag (mass fraction, %)

Fe_2O_3	SiO_2	Al_2O_3	ZnO	CaO	MgO	Na_2O	K_2O	SO_3	PbO	CuO	As_2O_3	TiO_2
52.04	34.51	3.32	2.59	2.33	1.26	1.06	0.64	0.50	0.45	0.30	0.28	0.22

reduction method, the research on the reduction of copper slag to recover iron has been paid more and more attention by researchers from all over the world in recent years, due to the rising price of iron ore. At present, the reduction temperature, reduction time, C/O ratio, and magnetic separation of copper slag have been fully researched, and metal iron products with iron content ≥ 90% have been obtained under laboratory conditions [8–13]. But there are few studies on the kinetics of iron reduction in slag, especially the reduction kinetics of copper slag-biomass composite pellets. Biomass comes from agricultural and forestry wastes, which can be prepared into biomass carbon after pyrolysis. Therefore, compared with traditional reducing agents such as coal, coke, heavy oil, and natural gas, biomass carbon not only has renewable characteristics but also has the advantages of wide distribution and ecological and environmental protection. In the future, the use of biomass carbon as a reducing agent is expected to reduce the operating cost of copper slag reduction to recover iron. At present, the reduction mechanism of copper slag-biomass composite pellets is not yet fully understood by researchers. Therefore, the research on the reduction kinetics of copper slag-biomass composite pellets is not only helpful to grasp the reduction mechanism, but also of great significance to guide industrial design and production.

The composition and structural characteristics of copper slag determine the complexity of the reduction process. In this paper, using biomass carbon as a reducing agent, an isothermal reduction experiment of CSBCP was carried out, the quality changes during the reduction process were recorded, and the kinetic analysis was carried out to explore the limiting links in the reduction process of copper slag biomass carbon.

2 Experimental

2.1 Materials

The copper slag sample was obtained from a copper company in Chinalco. The copper slag was crushed and ground to ~ 0.178 mm as the experimental material. The chemical composition of the copper slag is shown in Table 1, and its phase composition is shown in Fig. 1. It can be seen that fayalite (Fe_2SiO_4), magnetite (Fe_3O_4), and chalcopyrite ($CuFeS_2$) are the main phases in the copper slag. In addition, there may be a few substances that were not detected. Biomass carbon was provided by Tianjin Yadeer Biomass

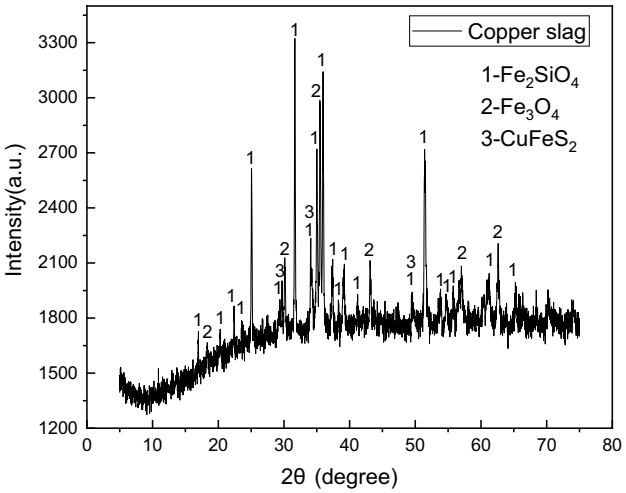

Fig. 1 X-ray diffraction spectrum of copper slag

Table 2 Main composition of biomass carbon (mass fraction, %)

Fixed carbon	Volatile matter	Ash	Moisture
76.51	5.28	10.81	7.40

Technology Co., Ltd. Its chemical composition is shown in Table 2, and the specific surface area of biomass carbon is 338.6 m^2/g. In order to ensure the full progress of the reaction, the biomass carbon is crushed and sieved, and the 0.15-mm sieve material is taken as the reducing agent.

2.2 Experimental Device and Method

Biomass carbon and copper slag were weighed according to the carbon–oxygen molar ratio (C/O = 1.2), and then a small amount of water was added to mix evenly and pressed into carbon-containing pellets with a size of Φ21 mm × Φ19 mm × 13 mm in a mold. The pressing pressure is 20 Mpa, and the holding time is 3 min. Finally, the sample was dried in an oven at 105 °C for 2 h to remove free water.

The isothermal direct reduction experiment of copper slag was carried out in a vertical tube furnace. Figure 2 shows the schematic diagram of a reduction experimental apparatus. An electric resistance furnace with six U-shape $MoSi_2$ heating elements was adopted to heat the samples. The inner diameter of the reactor tube was 50 mm, and the accuracy of the electronic balance was ± 0.001. In each isothermal reduction experiment, about 30 g of composite pellet samples was

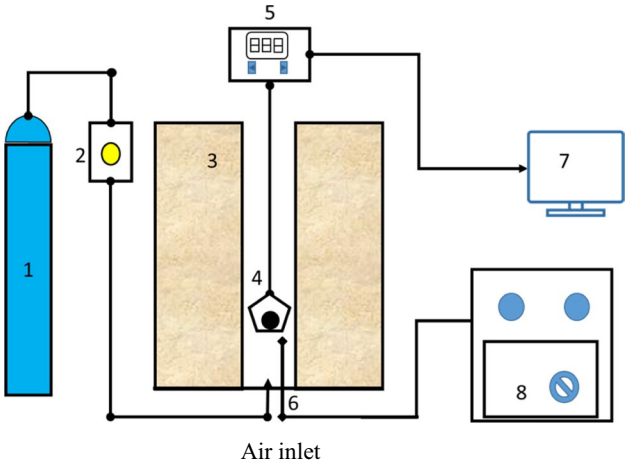

Fig. 2 Schematic diagram of isothermal reduction experimental device (1—argon cylinder, 2—flowmeter, 3—furnace, 4—molybdenum basket, 5—electronic balance, 6—Thermocouple, 7—data logging device, 8—temperature control device)

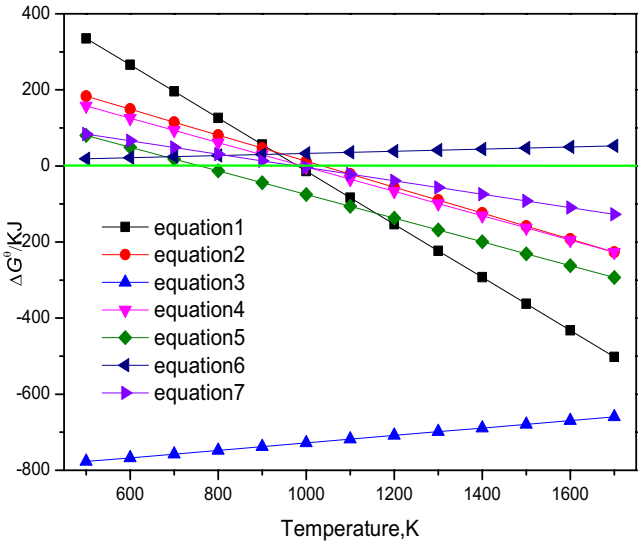

Fig. 3 The correlation of standard free energy with temperature for Eqs. (1–7)

loaded into molybdenum baskets. Argon was introduced into the bottom of the furnace tube at a flow rate of 0.5 L min^{-1}. When the temperature in the furnace was heated to the specified temperature (950 °C, 1000 °C, 1050 °C, 1100 °C, 1150 °C), the molybdenum basket containing the composite pellets was quickly hung under the electronic balance. The weight variation was monitored and recorded every 30 s. When the balance display remained at a certain value for more than 120 s, the reduction process was considered to be over. Then, stop heating and cool the pellets along with the furnace under an argon atmosphere.

3 Results and Discussion

3.1 Analysis of Copper Slag Reduction Process and Derivation of Reduction Fraction

The purpose of copper slag reduction is to convert iron-rich phases such as fayalite and magnetite in the copper slag into metallic iron. A series of reactions take place in the interior and surface of the pellets after heating, and the whole reduction process presents a multi-component interactive reaction. In the initial stage of pellet heating, the first reaction is the solid–solid reaction. During which, the iron-rich phase in the copper slag undergoes a direct reduction reaction with carbon particles. As the solid–solid reaction advances, the reducing gas CO generated by the reaction is in contact with the iron-containing material inside the pellet to undergo a reduction reaction during the diffusion (escape) process. In addition, the product of CO will also undergo a gas-solidification reaction with the carbon particles, namely, Boudouard reaction. The chemical reactions that may be involved in the reduction process of CSBCP are as follows [14–16]:

$$C + Fe_3O_4 = CO(g) + 3FeO \quad (1)$$

$$2C + Fe_2SiO_4 = 2CO(g) + 2Fe + SiO_2 \quad (2)$$

$$2CaO + Fe_2SiO_4 = 2FeO + 2CaO \cdot SiO_2 \quad (3)$$

$$C + FeO = CO(g) + Fe \quad (4)$$

$$2CaO + 2C + Fe_2SiO_4 = 2CO(g) + 2Fe + 2CaO \cdot SiO_2 \quad (5)$$

$$2CO + Fe_2SiO_4 = 2CO_2(g) + 2Fe + SiO_2 \quad (6)$$

$$CO_2 + C = 2CO \quad (7)$$

Thermodynamic calculation of reaction Eqs. (1–7) was carried out by using the thermodynamic calculation software HSC6.0, and the results are shown in Fig. 3.

Thermodynamic calculation shows that all the above can occur except reaction Eq. (6). According to the reaction formula (2), the starting temperature of the reaction between ferruginous olivine and carbon is 1036.7 K. When the reaction temperature rises, the lower standard Gibbs-free energy of the reaction can promote the formation of metal iron. In addition, according to the reaction formula (5), the starting temperature of the reaction between ferruginous olivine and carbon is reduced to 757.4 K, indicating that the introduction of CaO can reduce the decomposition temperature of ferruginous olives and promote the formation of metal iron in copper slag.

From the above chemical equation, it can be seen that the reduction weight loss of copper slag at high temperatures is mainly caused by the reduction of fayalite and iron oxides to generate CO and escape from the system. Therefore, the reduction fraction f can be calculated according to the change of pellet mass, as shown in Eq. (8):

$$f = \frac{\Delta W_t}{\Delta W_{\max}} = \frac{(W_0 - W_t)}{W_0 + W_c + W_v} \times 100\% \quad (8)$$

f is the reduction fraction, ΔW_t is the difference between the initial weight (g) of the pellet and the weight (g) at time t, $\Delta W_{\max}$ is the theoretical maximum weight (g) loss of the copper slag composite pellet, W_0 is the initial weight (g) of the pellet, and W_t is the weight (g) of the pellet at time t, W_O is the total oxygen atom weight (g) in the iron-containing compound, and W_C and W_V are the fixed carbon mass (g) and volatile matter mass (g) in the biomass carbon, respectively.

3.2 Determination of Copper Slag Reduction Reaction Model

According to the weight loss data of pellets at different temperatures, the relationship between reduction fraction f and reduction temperature and time is calculated by the Eq. (8), and the results are shown in Fig. 4.

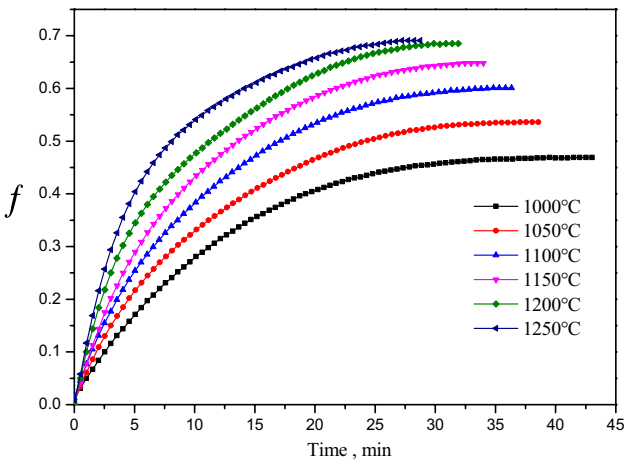

Fig. 4 The relationship between reduction fraction and time at different temperatures

Figure 4 shows that the reduction fraction f of copper slag-biomass composite pellets is positively correlated with both temperature and time. At 1000 °C, 1050 °C, 1100 °C, 1150 °C, 1200 °C, and 1250 °C, the reduction fractions f at the end of the experiment were 0.469, 0.536, 0.601, 0.648, 0.685, and 0.691, respectively. It can also be seen from Fig. 4 that after the red mud-biomass carbon composite pellets are reduced at 1200 °C for 30 min, the reduction fraction can reach more than 0.685, which provides a basic data for the research on the carbothermic reduction of copper slag biomass to recover iron.

4 Reaction Kinetics Analysis

4.1 Analysis of Speed Limit in Reduction Process

To explain the reduction mechanism and kinetics of iron minerals, numerous studies on the process of reducing iron minerals with solid carbon by thermogravimetry and other methods have been carried out, and different theoretical models of reaction rate control have been formed, as shown in Table 3.

To find out the limiting link of the reduction reaction of CSBCP, the above kinetic models were used to process the experimental data f. The data f at the end of the reaction and after the equilibrium is not meaningful for the fitting of the kinetic model. Therefore, in this experiment, the data between 0 and 0.95 $f_{\max}$ was selected for fitting ($f_{\max}$ is the reduction fraction at the reaction equilibrium). Figure 5 shows the relationship between the models (I ~ V) and time t respectively. Origin 8.5 software is used to perform linear fitting of different models, and the fitting results are shown in Table 4.

According to the fitting results in Table 4, the fitting coefficients of different models and the reaction rate constant k at the corresponding temperature can be known. By comparing the fitting coefficients of different models, it can be seen that the fitting degrees of models I and II are both above 0.99, and the fitting degree of model II is slightly better than that

Table 3 Kinetic mechanism function of reduction reaction [17–20]

Dynamics model	Model number	Reaction mechanism	Function, $G(f)$
Three-dimensional gas diffusion model	I	Three-dimensional, Jander equation (only applicable to the initial stage of reaction)	$kt=[1-(1-f)^{1/3}]^2$
	II	Three-dimensional, Ginstling-Brushtein equation	$kt=1-2/3f-(1-f)^{2/3}$
	III	Three-dimensional, G. Valensi-R. E. Carter equation	$kt=(1+f)^{2/3}-(1-f)^{2/3}$
Interfacial reaction	IV	Three-dimensional, shrink sphere	$kt=1-(1-f)^{1/3}$
Carbon gasification reaction	V	Boudouard reaction	$kt=-\ln(1-f)$

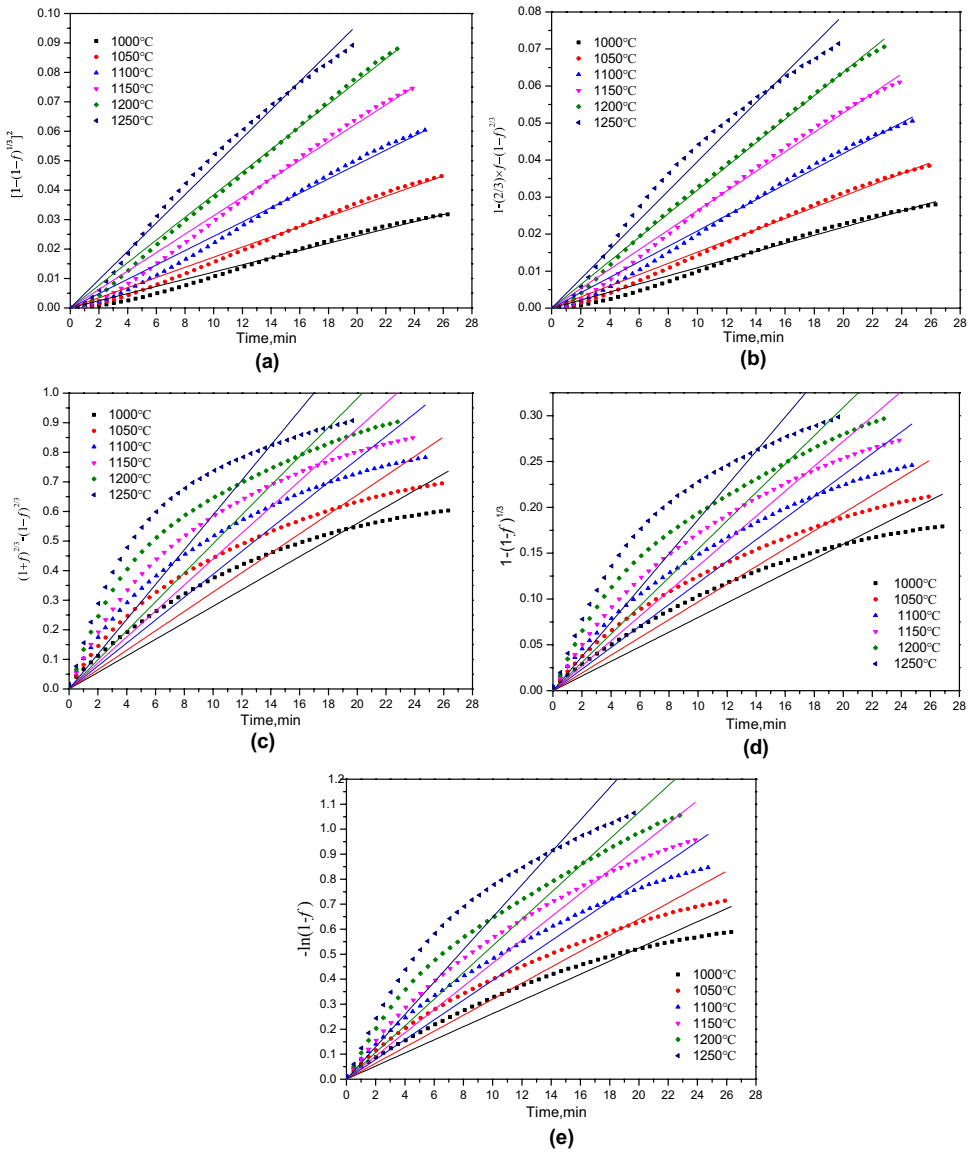

Fig. 5 Linear fitting of different reduction kinetic models. (**a**) [1-(1-f)1/3]2vs.time; (**b**) 1-2/3f-(1-f)2/3vs.time; (**c**) (1+f)2/3-(1-f)2/3vs.time; (**d**) 1-(1-f)1/3vs.time; (**e**) -ln (1- f) vs.time

of model I. Considering that model I is only applicable to the initial reaction [21], it is concluded that gas-phase diffusion is the limiting link in the reduction process of copper slag-biomass composite pellets, and its kinetic equation can be expressed by the Ginstling-Brushtein equation.

4.2 Calculation of Apparent Activation Energy in the Reduction Process

According to the rate constant k at different temperatures in Table 4, the apparent active method energy of the reduction reaction can be calculated using Arrhenius formula (9):

$$k = Aexp\left(-\frac{Ea}{RT}\right) \tag{9}$$

where A is the pre-exponential factor, s^{-1}; E_a is the apparent activation energy, J/mol; R is the ideal gas constant, 8.314 J/(mol K); T is the thermodynamic temperature, K.

Equation (10) can be obtained from Eq. (9). It can be seen from Eq. (10) that there is a linear relationship between ln$k$ and T^{-1}:

$$\ln k = -\frac{Ea}{R} \times \frac{1}{T} + \ln A \tag{10}$$

Bringing the rate constant k data of model II at different temperatures into the above formula, the linear regression curve of ln$k$ and $1/T$ can be drawn, as shown in Fig. 6. The pre-exponential factor A and the apparent activation energy E_a, calculated through the intercept and slope of the fitted straight line, are 2.782 s^{-1} and 82.67 kJ/mol, respectively. Apparent activation energy refers to the

Table 4 Results of the linear fitting under different kinetic models

Model	T, ℃	k, s^{-1}	Adj. R-Square
$[1-(1-f)^{1/3}]^2$	1000	1.22×10^{-3}	0.9944
	1050	1.73×10^{-3}	0.9964
	1100	2.43×10^{-3}	0.9961
	1150	3.13×10^{-3}	0.9969
	1200	3.35×10^{-3}	0.9989
	1250	4.81×10^{-3}	0.9973
$1-2/3f-(1-f)^{2/3}$	1000	1.09×10^{-3}	0.9957
	1050	1.51×10^{-3}	0.9978
	1100	2.09×10^{-3}	0.9978
	1150	2.64×10^{-3}	0.9982
	1200	3.19×10^{-3}	0.9994
	1250	3.96×10^{-3}	0.9948
$(1+f)^{2/3}-(1-f)^{2/3}$	1000	2.79×10^{-2}	0.9710
	1050	3.27×10^{-2}	0.9659
	1100	3.88×10^{-2}	0.997
	1150	4.39×10^{-2}	0.9645
	1200	4.91×10^{-2}	0.9613
	1250	5.88×10^{-2}	0.9525
$1-(1-f)^{1/3}$	1000	7.99×10^{-3}	0.9787
	1050	9.69×10^{-3}	0.9769
	1100	1.1177×10^{-2}	0.9774
	1150	1.36×10^{-2}	0.9759
	1200	1.545×10^{-2}	0.9699
	1250	1.866×10^{-2}	0.9585
$-\ln(1-f)$	1000	2.62×10^{-2}	0.9838
	1050	3.2×10^{-2}	0.9826
	1100	3.95×10^{-2}	0.9840
	1150	4.64×10^{-2}	0.9834
	1200	5.33×10^{-2}	0.9792
	1250	6.47×10^{-2}	0.9686

minimum energy required to convert reactant molecules into active molecules in a chemical reaction. It reflects how difficult a chemical reaction is to take place. Based on this, the reduction kinetics equation of CSBCP is calculated as follows:

$$1-2/3f-(1-f)^{2/3}=2.782\exp\left[-\frac{82670}{RT}\right]t \tag{11}$$

4.3 Effect of Temperature on Metallization Rate of Copper Slag Pellet

The content of metallic Fe and total Fe in the pellets after experiments at different temperatures (1100 ~ 1250 °C) was analyzed, and the metallization rate of the pellets was calculated as shown in Fig. 7. It can be seen that in the range of 1000–1200 °C, the metallization rate of the copper slag pellets increased rapidly with the increase of the heating temperature. This was because the reduction reaction of fayalite and iron oxides was an endothermic process; the increase of temperature was beneficial to promote the reduction reaction. In addition, the increase of temperature also helped to promote the gasification of carbon and the aggregation and growth of metallic iron. After the temperature exceeded 1200 °C, the temperature continued to rise, and the metallization rate decreased slightly. A reasonable explanation might be that a liquid phase was formed at high temperatures, which blocked the internal voids of the pellets and deteriorated the reaction conditions. Furthermore, some iron-containing phases or carbon particles may be surrounded by the liquid phase, which blocked the contact between the gas and solid phases, making it difficult to improve the metallization rate.

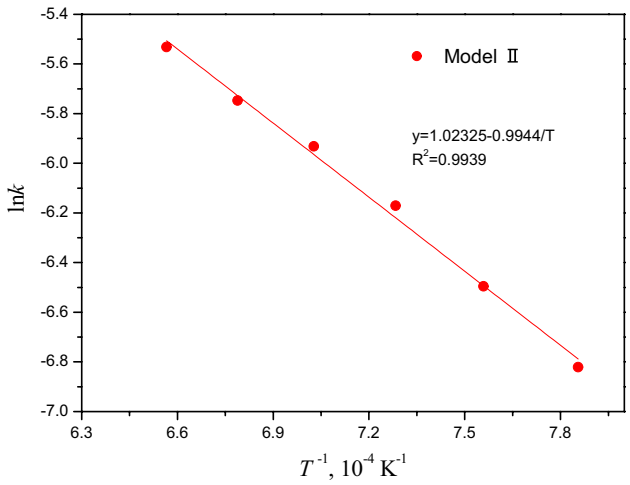

Fig. 6 Relationship between ln$k$ and $T.^{-1}$

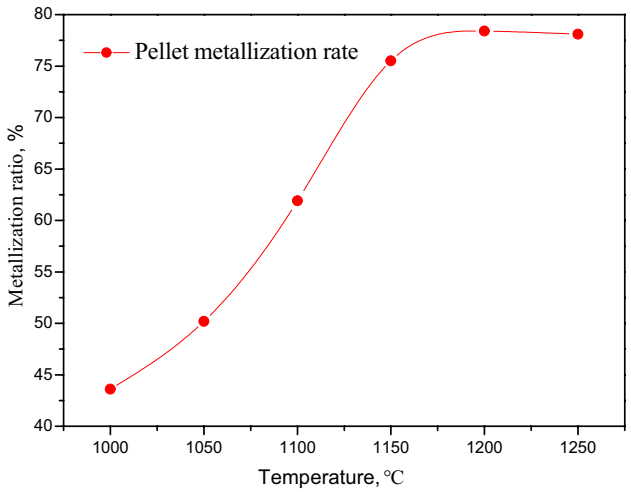

Fig. 7 Effect of temperature on metallization rate of pellet

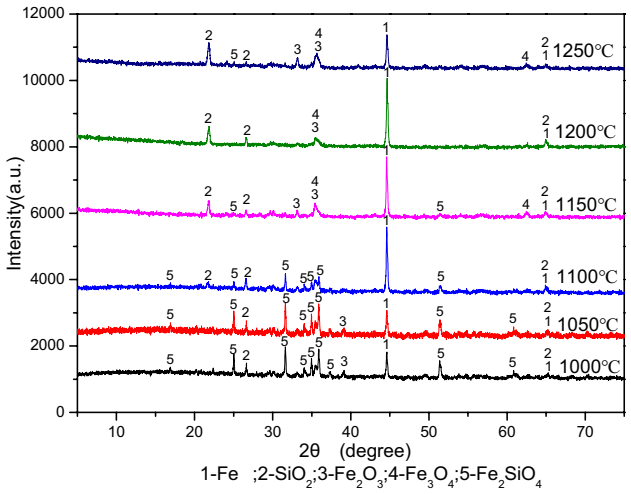

Fig. 8 XRD pattern of copper slag after reduction

The phase analysis of the reduced pellets was carried out, and the results are shown in Fig. 8. It could be seen that if the pellets reduced at 1000–1100 °C, they contained a large amount of fayalite phase, which indicated that the reduction of fayalite was insufficient under low-temperature conditions. After reducing at 1200 °C, the main phases were metallic iron, quartz, and a small number of iron oxides, which was consistent with the analysis of the metallization rate of the pellets. Therefore, the suitable reduction temperature of CSBCP was 1200 °C.

5 Conclusion

In this work, the isothermal reduction process of CSBCP was studied based on the weight-loss method, and the following conclusions were obtained:

1. It was technically feasible to reduce the iron-containing phase in copper slag by using biomass carbon as a reducing agent. The limiting link of the high temperature reduction of CSBCP was gas phase diffusion, the apparent activation energy of the reduction reaction was 82.67 kJ/mol, and its kinetic equation was

$$1 - 2/3f - (1 - f)^{2/3} = 2.782\exp\left[-\frac{82670}{RT}\right]t$$

2. The metallization rate of pellets was greatly affected by temperature, and the metallization rate of pellets increased rapidly from 43.6% to 78.4% with the increase of temperature from 1000 to 1200 °C. The suitable reduction temperature of copper slag-biomass composite pellets was 1200 °C, and the iron element in the reduction slag was mainly in the form of metallic Fe.

Funding 1. The National Key R&D Program "Solid Waste Recycling" key project "Integrated Demonstration of Solid Waste Collaborative Utilization in Key Industries in the Central Plains City Cluster in the Yellow River Basin" (2020YFC1908800);

2. Chinalco's independent research and development project: research on copper slag resource utilization technology based on carbothermal reduction (ZYY-2020-KJ-05).

3. Special fund project of Guangdong Academy of Sciences to build a domestic first-class research institution "Research on the regulation mechanism of enhanced interface separation of copper smelting slag" (2021GDASYL-202103059).

4. Guangzhou Science and Technology Plan Project "Study on Mechanochemical Effects of Low Temperature Sodification Process of Spent SCR Denitration Catalyst" (202102020372).

References

1. Huanosta-Gutiérrez T, Dantas RF, Ramírez-Zamora RM et al (2012) Evaluation of copper slag to catalyze advanced oxidation processes for the removal of phenol in water[J]. J Hazard Mater 213:325–330
2. Ambily PS, Umarani C, Ravisankar K et al (2015) Studies on ultra high performance concrete incorporating copper slag as fine aggregate[J]. Constr Build Mater 77:233–240
3. Zhang L, Zhu Y, Yin W et al (2020) Isothermal coal-based reduction kinetics of fayalite in copper slag[J]. ACS Omega 5(15):8605–8612
4. Lemougna PN, Yliniemi J, Adesanya E et al (2020) Reuse of copper slag in high-strength building ceramics containing spodumene tailings as fluxing agent[J]. Miner Eng 155:106448
5. Collins RJ, Ciesielski SK (1994) Recycling and use of waste materials and by-products in highway construction[M].
6. Shuai Li, Zeshuang K, Wanchao L (2021) Current situation and prospect of Cu slag treatment technology [J]. Spec Casting Nonferrous Alloy 41(03):289–293
7. Meshram P, Prakash U, Bhagat L et al (2020) Processing of waste copper converter slag using organic acids for extraction of copper, nickel, and cobalt [J]. Minerals 10(3):290
8. Geng C, Wang H, Hu W et al (2017) Recovery of iron and copper from copper tailings by coal-based direct reduction and magnetic separation[J]. J Iron Steel Res Int 24(10):991–997
9. Long H, Meng Q, Chun T et al (2016) Preparation of metallic iron powder from copper slag by carbothermic reduction and magnetic separation[J]. Can Metall Q 55(3):338–344
10. Sun Y, Gao P, Han Y et al (2013) Reaction behavior of iron minerals and metallic iron particles growth in coal-based reduction of an oolitic iron ore[J]. Ind Eng Chem Res 52(6):2323–2329
11. Zhang J et al (2015) A new technology for copper slag reduction to get molten iron and copper matte. J Iron Steel Res Int 22.5:396–401
12. Sarfo P et al (2017) Recovery of metal values from copper slag and reuse of residual secondary slag. Waste Manag 70:272–281
13. Li S et al (2019) A novel process to upgrade the copper slag by direct reduction-magnetic separation with the addition of Na2CO3 and CaO. Powder Technol 347:159–169
14. Zhao K, Gong XR, Li J et al (2016) Recovery of iron from copper slag by direct reduction, thermodynamics of copper and zinc [J]. J Environ Eng 10(5):2638–2646

15. Wang JP, Erdenebold U (2020) A study on reduction of copper smelting slag by carbon for recycling into metal values and cement raw material [J]. Sustainability 12(4):1421
16. Tang XY, Hu JH, Gao WG et al (2018) Characteristics of deep reduction of molten copper slag by bio-char [J]. J Cent South Univ (Nat Sci Ed) 7.
17. Ginstling AM, Brounshtein BI (1950) Concerning the diffusion kinetics of reactions in spherical particles[J]. J Appl Chem USSR 23(12):1327–1338
18. Prakash S, Ray HS (1990) Prediction of reduction kinetics of iron ore under fluctuating temperature conditions[J]. ISIJ Int 30(3):183–191
19. Haiyan C (2013) Study on catalytic steam gasification of biomass to syngas [D]. Huazhong Univ Sci Technol
20. Rao YK (1971) The kinetics of reduction of hematite by carbon[J]. Metall Trans 2(5):1439–1447
21. Li S, Kang Z, Liu W et al (2021) Reduction behavior and direct reduction kinetics of red mud-biomass composite pellets[J]. J Sustain Metall 7(1):126–135